*Asian Journal of Chemistry* Vol. 12, No. 1 (2000), 58–68

# Contribution to the Study of the Solar Evaporation of Sebkhat El Melah Brine (Tunisia)

A. M'NIF and R. ROKBANI*
*Laboratoire de génie des procédés*
*Institut National de recherche scientifique et Technique*
*B.P. 95-2050 Hammam Lif République tunisienne (Tunisia)*

A natural brine coming from Sebkhat El Melah can be assimilated to a quinary system: $Na^+$, $K^+$, $Mg^{2+}$, $Cl^-$, $SO_4^{2-}$ //$H_2O$. The study of the solar evaporation of our raw material can be based on the above-mentioned diagram. The practical crystallisation path is different from the theoretical one; however the recovered salts are similar to the foreseeable ones. Oversaturated solutions and metastable equilibrium may be the origin of the established gap.

## INTRODUCTION

Under appropriate conditions, it is economically interesting to recover potassium from a natural brine using solar evaporation. This way is limited by some parameters, especially by temperature which is low and variable. In the case of Sebkhat El Melah brine, this parameter varies between 15°C (cold season) and 40°C (hot season)[1].

To accomplish solar evaporation, a system of solar pans is usually used on an industrial scale[3–4]. The complexity of this system depends on the nature of the minerals to recover.

The aim of this study is to calculate, using quinary diagrams, the composition of the different salts in equilibrium with different solutions when a natural brine coming from « Sebkhat El Melah » is evaporated at 25°C. These theoretical results are thereafter compared with those obtained experimentally in a pilot pan ($2 \cdot 10^4$ $m^2$).

### Theoretical Path of Crystallisation

For theoretical calculations we use an isotherm at 25°C of the oceanic quinary diagram[2, 5–11] represented by Fig. 1. Using this diagram and to approach the real conditions of the field, we suppose for our calculations that the crystallised salts are removed from the solutions when the system reaches an equilibrium line or a third point. On the diagram (Fig. 1) the raw natural brine is represented by "z" which is situated in the field of the magnesium sulphate hexahydrate. At first, during evaporation the system does not move from z and will precipitate sodium chloride (salt No. 1). When the brine becomes saturated with magnesium sulphate (z′) (z and z′ are superposed) the system moves on [Bz] line and crystallises a

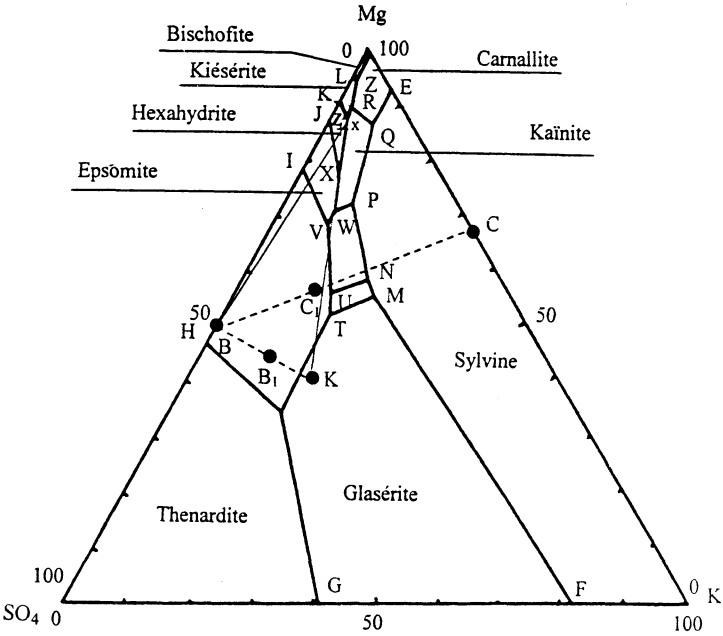

z = Natural brine of Sebkhat El Melah

Fig. 1. 25 °C isotherm of the oceanic quinary diagram

mixture of magnesium sulphate hexahydrate and sodium chloride, represented by B point; when «x» is reached (intersection point between [Bz] and [XY]), the crystallised salt is removed and the new system is represented by «x». X, Y and K (position of kaïnate salt in the diagram) are in line, it is not possible to across the field of kaïnate ($KCl\cdot MgSO_4\cdot 2.75H_2O$), the system will move on the border of this field and crystallise a mixture of sodium chloride and kaïnate until it reachs «Y». At this time we can remove the crystallised salt. Between «Y» and «R» we recover a mixture of sodium chloride, kaïnate and kieserite ($MgSO_4\cdot H_2O$) represented by «$B_1$». The new system represented by «R» point will move on [RZ] line to precipitate a mixture of sodium chloride, carnallite ($KCl\cdot MgCl_2\cdot 6H_2O$) and kieserite represented by «$C_1$». The «Z» point is a real invariant point; it represent a solution with a congruent saturation; if we continue evaporation the system does not move and all the water will be evaporated, and a mixture of sodium chloride, carnallite, kieserite and bischofite ($MgCl_2\cdot 6H_2O$) will crystallise.

This operating method will be adopted in order to recover three different salts, sodium chloride (NaCl), kaïnitic salt (mixture of salts containing kaïnite) and carnallitic salt (mixture of salts containing carnallite). The cutting points are «z′» recovery of NaCl, «R» recovery of kaïnitic salt and «Z» recovery of carnallitic salt. The operating flow diagram is given by Fig. 2.

The compositions at the different cutting points (z′, R, Z) are calculated using the quinary diagram saturated with NaCl at 25°C and the concentrations table, deter-

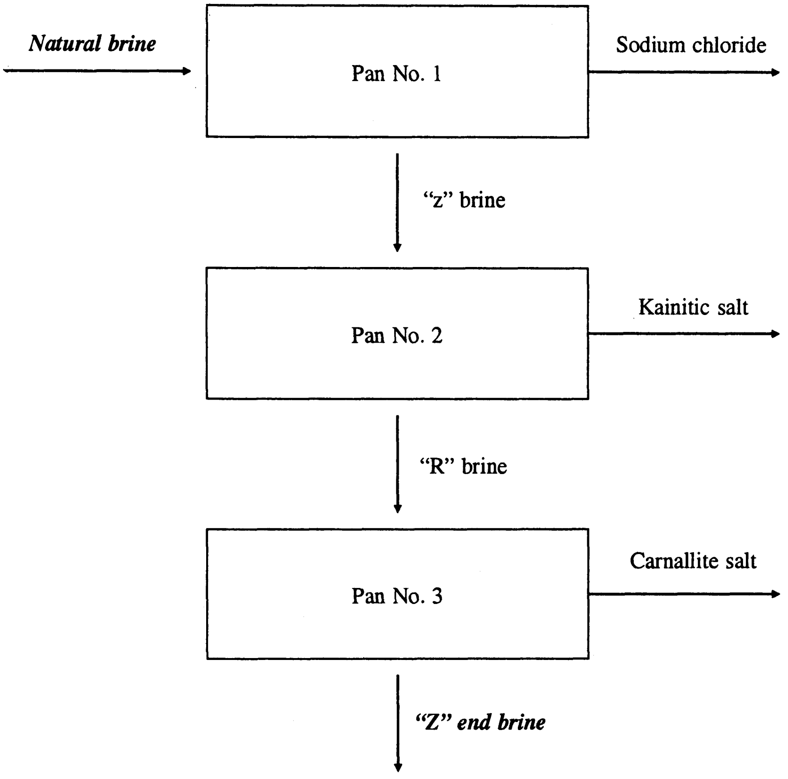

Fig. 2. Operating flow diagram

mined by d'Ans, at the same temperature[1, 8, 9]. Table-1 shows the compositions of these points.

TABLE–1
BRINE COMPOSITIONS AT THE CUTTING POINTS (moles/1000 moles $H_2O$)

| | Raw brine (z) | z′* | R | Z |
|---|---|---|---|---|
| $Na_2Cl_2$ | 18.40 | 3.35 | 1.70 | 0.60 |
| $K_2Cl_2$ | 1.90 | 3,53 | 2.50 | 0.90 |
| $MgCl_2$ | 38.64 | 71,63 | 85.50 | 102.00 |
| $MgSO_4$ | 6.66 | 11,98 | 8.00 | 5.50 |
| $H_2O$ | 1000 | 1000 | 1000 | 1000 |

(*)Saturated with magnesium sulphate hexahydrate.

Fig. 3 shows the graphical representation of the concentration evolution regarding the evolution of $MgCl_2$ concentrations.

Three sequences of crystallisation are shown by this figure. A theoretical balance, for the isothermal evaporation at 25°C based on the mentioned cutting points, is given hereafter (initial condition is equivalent to 1000 moles $H_2O$).

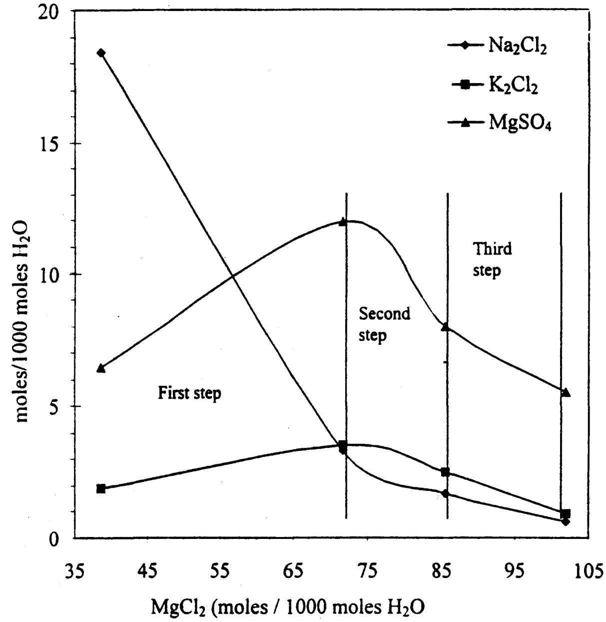

Fig. 3. Theoritical Concentrations of different salts as a function of $MgCl_2$ concentrations

## First step: Crystallisation of sodium chloride

From «z» (raw brine) to «z′» sodium chloride (salt No. 1) will crystallise. During this phase we crystallise 90% of total sodium chloride and evaporate 46% of initial water. Table-2 shows the calculated results.

TABLE–2
QUANTITY AND COMPOSITION OF THE CRYSTALLISED SALTS

| | Initial (moles/1000 moles $H_2O$) | Final | moles | Concentration (%) | ratio (%) |
|---|---|---|---|---|---|
| $Na_2Cl_2$ | 18.397 | 3.35 | 16.59 | 100 | 90% |
| $K_2Cl_2$ | 1.904 | 3.529 | — | — | — |
| $MgCl_2$ | 38.64 | 71.634 | — | — | — |
| $MgSO_4$ | 6.459 | 11.975 | — | — | — |
| $H_2O$ | 1000 | 1000 | 460.59 | — | 46% |

## Second step: Crystallisation of Kaïnitic salt

After removing the crystallised sodium chloride salt, evaporation continues to «R». A mixture of three salts (salt No. 2) will crystallise: NaCl, kaïnate and kieserite. During this step 5.65% of total initial sodium chloride crystallise, 20% of initial sulphate ions crystallise as kieserite, 40.64% of initial potassium ions crystallise as kaïnite and 8.75% of initial water is removed. Table-3 shows the calculated results.

TABLE-3
QUANTITY AND COMPOSITION OF THE CRYSTALLISED SALTS

| Compose | Weight (g) | Concentration (%) | Ratio (%)* |
|---|---|---|---|
| $Na_2Cl_2$ | 121.53 | 17.90 | 5.65 |
| $MgSO_4$ | 179.33 | 26.41 | 20.07 |
| Kainite ($KCl·MgSO_4·3H_2O$) | 378.08 | 55.69 | 40.64† |
| Total | 678.94 | 100 | — |

*Ratio (%), compared to initial quantity in the natural brine.
†Compared to initial KCl in the natural brine.

## Third step: Crystallisation of Carnallitic Salt

After removing the crystallised mixture of salts (salt No. 2) evaporation continues between «R» and «Z»; a mixture of three salts crystallises (NaCl, kieserite, and carnallite: salt No. 3) In this case 3% of total initial sodium chloride crystallises, 25% of initial sulphate ions crystallise as kieserite and 42.18% of initial potassium ions crystallise as carnallite. The calculated results are recapitulated in Table-4.

TABLE-4
QUANTITY AND COMPOSITION OF THE CRYSTALLISED SALTS

| Compose | Weight (g) | Concentration (%) | Ratio (%) |
|---|---|---|---|
| $Na_2Cl_2$ | 64.40 | 8.77 | 2.99% |
| Kieserite ($MgSO_4·H_2O$) | 223.87 | 30.48 | 25.06% |
| Carnallite ($KCl·MgCl_2·6H_2O$) | 446.21 | 60.75 | 42.18%(*) |
| Total | 734.48 | 100.00 | — |

*Ratio in% = percentage of initial KCl crystallised into carnallite form.

In practice (industrial scale) this crystallisation path is subject to some modifications which can meet their origin in the considerations hereafter:

The solutions are not continuously at equilibrium.

The temperature is not constant.

With regard to these considerations, it seems to be interesting to refer to experimental results (pilot scale), to draw the crystallisation path and to make a material balance which reflects a better picture of the industrial situation.

Before giving the experimental results we think that it is useful to expose a summary about the meteorological data at Sebkhat El Melah of Zarzis.

## Meteorological Conditions at Sebkhat El Melah of Zarzis

The climate at Sebkhat El Melah of Zarzis is characterised by two seasons:

(a) A hot season (May–September), (b) A cold season (October–April).

The average conditions for these two seasons are calculated from the data collected on the site of the Sebkhat and summarised in Table-5.

TABLE-5
AVERAGE CONDITIONS FOR THE TWO SEASONS*

| Climatic parameters* | Hot season | Cold season |
|---|---|---|
| Average temperature | 27.5°C | 15.6°C |
| Hygrometry | 70% | 67% |
| Wind velocity : 8H00 | 3.5 m/s | 3.7 m/s |
| : 18H00 | 6.3 m/s | 4.8 m/s |
| Evaporation rate (fresh water) | 8 mm/day | 4 mm/day |
| Rain (mm/y) | 75 mm/year | |

*Internal reports, ONM (Tunisia)

Knowing that the evaporation rate depends on the specific gravity of brine we have done some experiments to determine a correlation between the density of brine (d) and the evaporation rate ($\tau$). For our calculations we consider that the evaporation rate for fresh water is equal to one (8 mm/day). Fig. 4 represents the average evaporation ratio calculated from data collected on the site. This curve seems to satisfy the following equation:

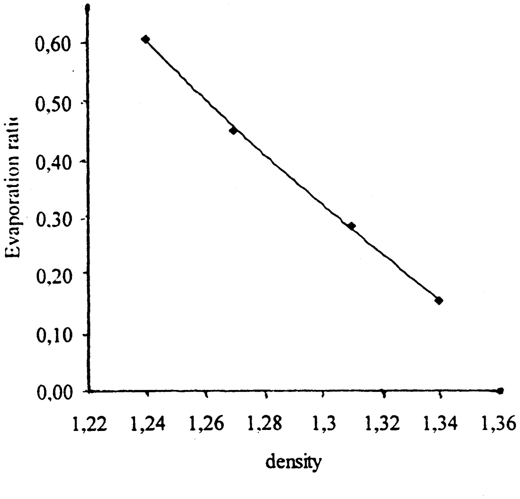

Fig. 4. Evaporation Ratio depending in the temperature

$$\tau = 5.5556d^2 - 18.807d + 15.384 \quad (1.240 \leq d \leq 1.340)$$

Using this equation it is possible to assess the evaporation rate for any evaporated brine coming from Zarzis natural brine which may help in engineering calculations of the pans area.

## EXPERIMENTAL

A pilot unit of solar pans is used for this study on the site of Sebkhat El Melah. A pump of 250 $m^3$/h is used to feed the pilot unit with natural brine. The transfer of the brine from one pan to the other is performed by gravity; sometimes a circulating pump is used for help. The parameter density is used as an indicator for the transfer. The medium flow rate of natural brine is 50 $m^3$/h and the total pumped volume is 20000 $m^3$/year.

The flow diagram shown in Fig. 2 is used to perform the work. The daily controlled parameters are:

Temperature, evaporation rate, hygrometry, velocity and direction of wind.

Density in each pan (input and output).

Brine sampling from each pan (input and output).

Salt sampling.

The collected samples are analysed daily.

## RESULTS AND DISCUSSION

Under the above mentioned conditions, a pilot solar evaporation test is done on the site. For this purpose a system of four pans is used. The total area of these pans is 2000 $m^2$. The cutting densities used to perform the pilot evaporation test are respectively at the end of each pan 1.250 (first pan), 1.270 (second pan), 1.305 (third pan) and 1.340 (fourth pan). The cutting densities are determined further by orientation tests. The objective consists in crystallising sodium chloride in the two first pans (salt No. 1, Fig. 2), kaïnitic salt in the third pan (salt No. 2 and carnallitic salt in the fourth pan (salt No. 3).

Experimental results are summarised in Table-6 for solutions and Table-7 for solids.

TABLE-6
BRINE COMPOSITION AT THE CUTTING DENSITY

| | ION | | | | | | | | |
|---|---|---|---|---|---|---|---|---|---|
| pan | $SO_4^{2-}$ | $Ca^{2+}$ | $Mg^{2+}$ | $K^+$ | $Na^+$ | $Br^-$ | $Cl^-$ | $H_2O$ | Cutting density |
| SN | 30.74 | 0.72 | 54.37 | 7.36 | 41.95 | 3.20 | 208.70 | 892.26 | 1.2393 |
| Pan 1 | 33.12 | 0.50 | 61.59 | 7.75 | 34.72 | 3.62 | 205.71 | 903.39 | 1.2504 |
| Pan 2 | 39.32 | 0.49 | 77.40 | 9.60 | 22.00 | 4.30 | 223.01 | 894.18 | 1.2703 |
| Pan 3 | 47.44 | 0.27 | 89.91 | 11.45 | 10.91 | 5.16 | 248.37 | 886.79 | 1.3003 |
| Pan 4 | 51.71 | 0.00 | 105.17 | 3.02 | 3.77 | 6.50 | 276.70 | 886.93 | 1.3338 |

TABLE-7
IONIC SALT COMPOSITIONS IN THE DIFFERENT PANS IN (%)

| Pan | $SO_4^{2-}$ | $Ca^{2+}$ | $Mg^{2+}$ | $K^+$ | $Na^+$ | $Cl^-$ | $H_2O$ |
|---|---|---|---|---|---|---|---|
| 1* | 0.79 | 0.12 | 0.97 | 0.13 | 36.09 | 57.44 | 4.46 |
| 2* | 1.12 | 0.30 | 1.08 | 0.12 | 35.21 | 57.85 | 4.32 |
| 3 | 1.63 | 0.38 | 1.68 | 0.25 | 34.27 | 56.73 | 5.06 |
| 4 | 4.83 | 0.16 | 7.74 | 8.51 | 8.00 | 39.96 | 30.80 |

*Salt No. 1

(a) *Evolution of brine*: To make the comparison more easy we convert the result of Table-6 into moles/1000 moles $H_2O$, and we trace the evolution of each salt regarding the number of moles $MgCl_2$. Table-8 and Fig. 5 show the obtained results.

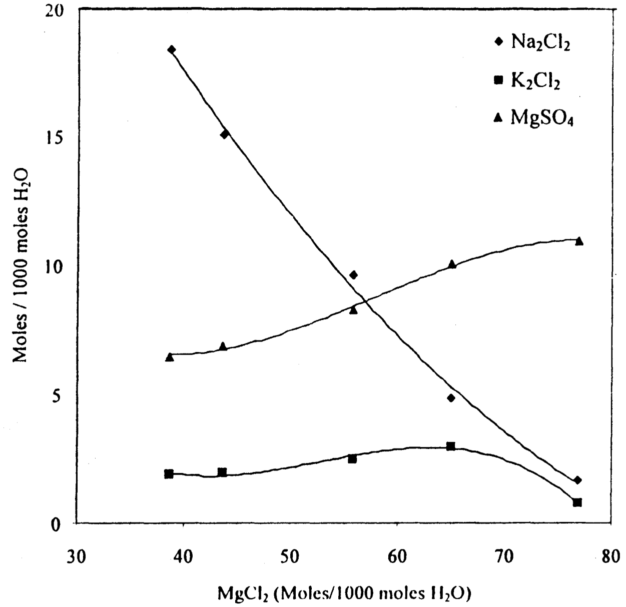

Fig. 5. Practical Concentrations of different salts as a function of $MgCl_2$ concentrations

Using these results we draw the crystallisation path of the brine during solar evaporation on the quinary diagram. Fig. 6 shows this path.

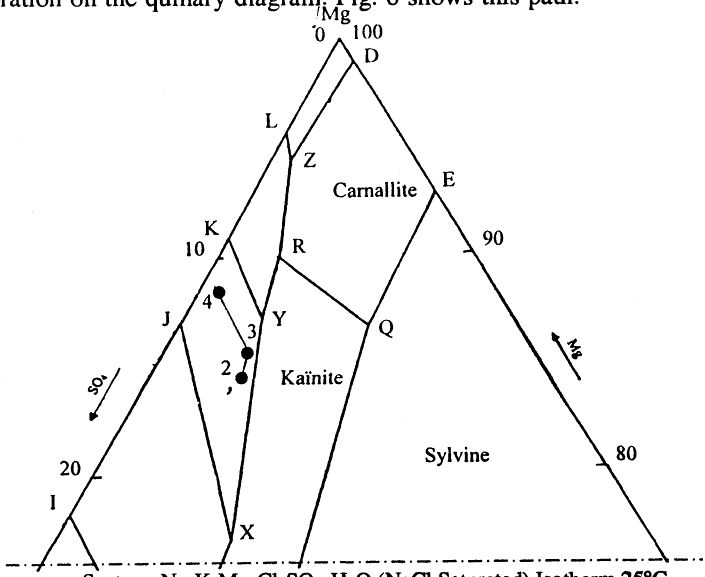

System: Na-K-Mg-Cl-$SO_4$-$H_2O$ (NaCl Saturated) Isotherm 25°C

z = Natural brine, 2 = Brine out pan 2, 3 = Brine out pan 3, 4 = brine out pan 4(end brine)

Fig. 6. Practical crystallisation path

The practical path of crystallisation (Fig. 6) is different from the theoretical one. The compositions of different brines (Table-8) disagree with the calculated ones (Table-1). If we compare the theoretical solutions R and Z (Table-1) respectively with the practical solutions out of pans 3 and 4 (Table-8), we note that the real solutions are richer in $MgSO_4$ and poorer in $MgCl_2$; however $K_2Cl_2$ is about the same. If we compare the evolution of the theoretical concentrations (Fig. 3) to the practical concentrations (Fig. 5), we note that the curve representing $MgSO_4$ remains almost constant and does not decrease. Also we can expect that the recovered salts (salt No. 2 and Salt No. 3 will contain less $MgSO_4$ than the calculated ones. As a consequence of the above mentioned remark, the positions of the real solutions on the diagram are out of the foreseen fields (Fig. 6).

TABLE-8
PRACTICAL BRINE COMPOSITION IN MOLES/1000 MOLES $H_2O$

| mole/1000 moles $H_2O$ | $MgCl_2$ | $Na_2Cl_2$ | $K_2Cl_2$ | $MgSO_4$ |
|---|---|---|---|---|
| SN | 38.64 | 18.40 | 1.90 | 6.46 |
| Pan 1 | 43.59 | 15.04 | 1.98 | 6.87 |
| Pan 2 | 55.82 | 9.63 | 2.48 | 8.24 |
| Pan 3 | 65.01 | 4.81 | 2.98 | 10.03 |
| Pan 4 | 76.83 | 1.66 | 0.79 | 10.93 |

The established differences meet their origins particularly in two effects:

The temperatures which are not constant.

The kinetics of the formation and dissolution of the salts.

The salts that crystallise by evaporation have often velocity of formation and of dissolution very different. This is again true when we obtain double sulphated salts. Some other salts could not crystallise and they need the addition of germs. The phenomena we mentioned are generally the origin of the apparition of metastable and oversaturated solutions.

The obtained results indicate that the processed solutions are metastable, richer in sulphate ions, for a given content in magnesium ion, at equilibrium.

(c) *Nature of crystallised salts*: The ionic compositions of the recovered salts are shown in Table-7. We have calculated at first the medium ionic composition of the salt No. 1 (pan 1 and 2). In the next step we calculated the hypothetical mineralogy composition for each salt. The obtained results are recapitulated in Table 9.

The salt No. 1 contains 98% NaCl when it is dry. The presence of less than 2% of potassium, magnesium and sulphate in this salt is due to the coated solution of the crystals. It is comparable to the foreseeable salt from the diagram of oceanic quinary system at 25°C (Table-2).

The real composition of salt No. 2 is very different from the calculated composition (Table-3). This salt contains 95% NaCl, 2.6% $MgSO_4 \cdot 6H_2O$ and

TABLE-9
MINERALOGICAL COMPOSITIONS OF THE RECOVERED SALTS

| | Salt No 1 | | | Salt No 2 | | | Salt No 3 | | |
|---|---|---|---|---|---|---|---|---|---|
| | Mole | Weight (g) | % sec | Mole | Weight (g) | % sec | Mole | Weight (g) | % sec |
| Gypsum | 0.005 | 0.714 | 0.772 | — | — | — | — | — | — |
| NaCl | 1.550 | 90.675 | 98.068 | 1.490 | 87.165 | 95.604 | 0.348 | 20.348 | 20.606 |
| $MgSO_4 \cdot 6H_2O$ | 0.005 | 1.073 | 1.160 | 0.011 | 2.413 | 2.647 | — | — | — |
| Kiésérite | — | — | — | — | — | — | 0.031 | 4.245 | 4.299 |
| Kaïnite | — | — | — | 0.006 | 1.595 | 1.749 | 0.020 | 4.882 | 4.944 |
| Carnallite | — | — | — | — | — | — | 0.199 | 55.170 | 55.870 |
| $MgCl_2 \cdot 6H_2O$ | — | — | — | — | — | — | 0.069 | 14.102 | 14.281 |
| Total | | 92.462 | 100 | | 91.173 | 100 | | 98.748 | 100 |
| Humidty | 100 | 7.538 | — | 100 | 8.827 | — | 100 | 1.252 | 1.268 |

1.7% Kaïnite. The less percentage of this salt in kaïnite and magnesium sulphate is probably due to the oversaturation of this type of solutions. This hypothesis is confirmed when we examine the evolution of $SO_4^{2-}$ (Fig. 5). This ion does not crystallise when we evaporate the brine. Neitzel[10] explains this phenomenon by the formation of oversaturated solutions. Without this phenomenon this salt might be rich in kaïnite and used as raw material for producing $K_2SO_4$.

The obtained salt No. 3 is a real carnallitic salt (55.8% carnallite). Compared to the theoretical salt No. 3 (Table-4) it contains 5% kaïnite, 4.3% kieserite and 14% bischofite ($MgCl_2 \cdot 6H_2O$). The presence of kaïnite and bischofite in this salt is probably attached to the cutting densities and temperature fluctuations. Kaïnite must crystallise with salt No. 2 and bischofite will be rejected with the end brine. A particular attention should be paid to these impurities because they cause a lot of problems when the carnallitic salt is treated for producing KCl. However, the kiesirite represents 4.3% instead of 30.5% (theoretical rate). As mentioned above, this phenomenon is attached to the formation of oversaturated solutions.

## Conclusion

The obtained results disagree noticeably with theoretical forecasting got from the quinary diagrams. Some associated effects contribute to create the gap between theory and practice. We mention particularly the meteorological conditions, the choice of cutting densities and especially the presence of $MgSO_4$ in the brine which becomes oversaturated, and allows metastable equilibrium.

## REFERENCES

1. A. M'nif, Thèse de doctorat de spécialité, Fac. Sc., Tunis (June 1984).
2. J D'ans, Untersuchungen über metastabile löslichkeiten in system der salze ozeanischer Salzablagerungen, Kali, pp. 38, 42–49, 69–73, 86–92, 181–185 (1944).
3. S. Pancharatnam, *Desalination*, **11**, 303 (1972).

4. Joseph A. Epstein, *Chemistry and Industry*, 16 (1977).
5. R. Berthon and A. Aubry, *Revue de chimie minérale*, **7**, 231 (1970).
6. L. Zayani, A. M'nif, R. Rokbani, R. Cohen-Adad and M.T. Cohen-Adad, XXIIIème Jeep, Hammamet, Tunisie, p. 129 (1997).
7. C. Djebali, L. Zayani, A. M'nif and R. Rokbani, XXIIIème Jeep, Hammamet, Tunisie, p. 35 (1997).
8. Shumpel Oka, On reliability of graphical calculation of ionic brine evaporation.
9. Linke, Solubilities of Inorganic and Metal Organic Compounds. VolumeII, 4th Edn., Am Chem Soc.,
10. Ulrich Neitzel, Kristallisation von salzen aus den laugen des Gro Ben Salzsees in theorie und praxis, Kali und Steinsals Vol. 10 (January 1971).
11. O. Karsten, *Z. Anorg Allg. Chem.*, **263**, 292 (1950).

(*Received*: 15 June 1999; *Accepted*: 27 September 1999) AJC–1851